ELSEVIER

Slime mold microfluidic logical gates

Andrew Adamatzky[1,*] and Theresa Schubert[2]

[1] University of the West of England, Bristol, UK
[2] Bauhaus-University Weimar, Germany

We demonstrate how logical operations can be implemented in ensembles of protoplasmic tubes of acellular slime mold *Physarum polycephalum*. The tactile response of the protoplasmic tubes is used to actuate analogs of two- and four-input logical gates and memory devices. The slime mold tube logical gates display results of logical operations by blocking flow in mechanically stimulated tube fragments and redirecting the flow to output tube fragments. We demonstrate how XOR and NOR gates are constructed. We also exemplify circuits of hybrid gates and a memory device. The slime mold based gates are non-electronic, simple and inexpensive, and several gates can be realized simultaneously at sites where protoplasmic tubes merge.

Introduction

The plasmodium of *Physarum polycephalum* (Order *Physarales*, class *Myxomecetes*, subclass *Myxogastromycetidae*) is a single cell, visible with unaided eye, with many diploid nuclei. The plasmodium feeds on bacteria and microscopic food particles by endocytosis. When placed in an environment with distributed sources of nutrients the plasmodium forms a network of protoplasmic tubes connecting the food sources. The slime mold develops a network of protoplasmic tubes spanning sources of nutrients, and the cell maintains its integrity by pumping nutrients and metabolites between remote parts of its body via cytoplasmic streaming [1–6].

Cytoplasmic streaming could be employed for the transportation of bio-compatible substances inside the protoplasmic network. In [7] we demonstrated that the plasmodium of *P. polycephalum* consumes various colored dyes and distributes them in its protoplasmic network. By specifically arranging a configuration of attractive (sources of nutrients) and repelling (sodium chloride crystals) fields we can program the plasmodium to implement the following operations: to take in specific colored dyes from the closest colored oat flake; to mix two different colors to produce a third color; and, to transport color to a specified locus of an experimental substrate. Inspired by our previous results [7] and studies on cellular endocytosis of magnetic nano-beads [8] and fluorescent nano-beads [9], and intake of latex beads by the amoeba's endocytotic mechanisms [10], we undertook experiments on the intake of magnetite nanoparticles and glass micro-spheres coated with silver metal by Physarum [11]. We found that the slime mold can propagate the nanoscale objects using a number of distinct mechanisms, including endocytosis, transcytoses and dragging.

The protoplasmic networks developed by *P. polycephalum* are living, self-growing microfluidic systems [12–14] capable of intake and controlled delivery of biocompatible materials. The slime mold microfluidic systems can range in size from a few millimeters to meters of complex protoplasmic networks with hundreds of interconnected tube fragments. To be used efficiently the protoplasmic networks must be controlled and the flow of cytoplasm transporting objects must be programmed.

Laboratory prototypes of microfluidic control devices are based on bubble valves [15], droplet and bubble gates [16,17], embedded valves with pressure-dependent states [18], coupling microfluidic systems with electronic chips [19,20], tension-based passive pumping and fluidic resistance gates [21] and devices based on a fluid's rheological properties [22,23]. These are not efficient, and most of them are not applicable, when dealing with a living slime mold microfluidic system.

In 2004, Vestad, Marr and Munakata [13,24] constructed logical gates by changing the functional properties of a fluidic system without requiring non-linear properties of a liquid. They showed that by dynamically changing the resistance of individual channels in a microfluidic system it is possible to direct the overall system of

*Corresponding author:. Adamatzky, A. (andrew.adamatzky@uwe.ac.uk)

 http://dx.doi.org/10.1016/j.mattod.2014.01.018

relative flow rates, independent of the pressure of the liquid. Their logical gates are actuated by depressing one channel of the system and reconfiguring the network [24]. Being inspired by the Vestad–Marr–Munakata results we conducted laboratory experiments with slime mold *P. polycephalum* and found that when a fragment of a protoplasmic tube is mechanically stimulated, a cytoplasmic flow in this fragment halts and thus resistivity increases. The cytoplasmic flow is then directed through adjacent protoplasmic tubes. We explored this phenomenon to construct several logical gates and a memory device.

Methods

Plasmodium of *P. polycephalum* was cultivated in plastic containers, on paper towels sprinkled with distilled water and fed with oat flakes (Alnatura Haferflocken, Feinblatt, Germany). The experimental substrate was 2% non-nutrient agar gel (Agar-Agar, Kobe I, pulverized. Carl Roth, Germany) poured in 9 cm plastic Petri dishes. In each experiment an oat flake colonized by a plasmodium was placed in the center of the Petri dish. Protoplasmic tubes were mechanically stimulated with a human hair approximately 50 μm in diameter, 4–5 cm in length. During actuation of a protoplasmic tube fragment, a tip of hair was forced into a wall of the tube until temporary invagination of the wall and/or immediate stoppage of cytoplasmic flow occurred. Videos of cytoplasmic flows were recorded using digital high-resolution microscope Keyence VH-Z20R (KEYENCE Microscope Europe) at zoom 200×.

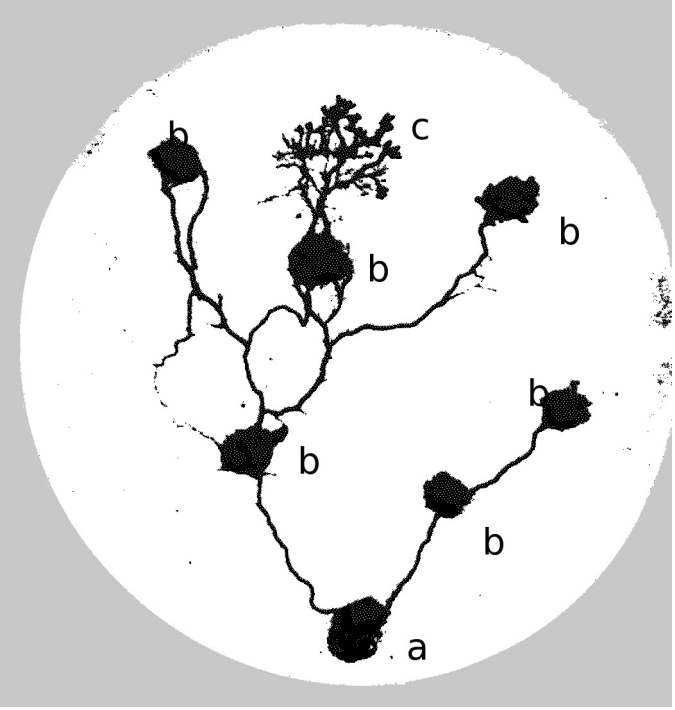

FIGURE 1

Example of a Physarum tree. Inoculation site is labeled 'a', oat flakes acting as sources of nutrients are 'b' and a growing zone is 'c'. Physarum grows in a 9 cm Petri dish, shown as a white disk.

Results

After being inoculated on an agar gel, the slime mold *P. polycephalum* grows on the substrates. On a nutrient substrate the slime mold grows similarly to excitation waves in a non-linear excitable medium. On a non-nutrient substrate Physarum exhibits localized growth zones, similar to self-localized traveling excitations, propagating on the substrate away from the original inoculation site, see details in [25]. The active growth zones are subjected to internal instabilities and therefore divide periodically. Thus a growing and branching tree of protoplasmic tubes emerges from the inoculation zone (Fig. 1).

An undisturbed Physarum exhibits more or less regular patterns of oscillation of its surface electrical potential. The electrical potential oscillations are likely controlling the peristaltic activity of protoplasmic tubes, necessary for the distribution of nutrients in the spatially extended body of Physarum [26,27]. A calcium ion flux through the membrane triggers oscillations responsible for the dynamics of contractile activity [28,29]. The Physarum surface electrical potential oscillates with an amplitude of 1–10 mV and a period of 50–200 s, associated with shuttle streaming of cytoplasm [29–32]. Oscillations of the electrical potential and the corresponding peristaltic activity are due to calcium waves propagating along protoplasmic tubes. These waves, and the associated electrical charges, plus the difference in electrical potential leads to a flow of cytoplasm.

In any given tube cytoplasmic flow reverses its direction every circ. 54 s (Table 1). We can speculate this is because calcium and peristaltic waves propagate from a root (inoculation site) of a Physarum tree toward its leaves (growth zones) and then back. That is, a protoplasmic tree is polarized and its polarization is reversed almost every minute.

When a segment of a protoplasmic tube between two junctions or branching points, is touched with a hair, a flow of cytoplasm inside this fragment becomes blocked. The cytoplasmic flow blocking could be due to K^+ channel activation, increases in intracellular Ca^{2+}, temporary increases in concentration of inositol trisphosphate, activation of adenylyl cyclase, see overviews in [33,34]. A mechanically stimulated fragment restores its conductivity and the flow of cytoplasm in 54–59 s after the stimulation (Table 1).

When a fragment of a tube becomes blocked, the flow of cytoplasm is directed through auxiliary, or second-order, bypassing tubes. The main, or first order, protoplasmic tubes have diameters approx. 100 μm while auxiliary, second order, tubes have diameters of 30–40 μm. In intact Physarum trees, the flow of cytoplasm is directed along a route with the lowest resistance, i.e. along first-order tubes whose diameter is large. Tubes with a

TABLE 1

Period of reversing flow in protoplasmic tubes (21 experiments) and recovery time after mechanical stimulation (12 experiments).

	Flow reversing period (s)	Recovery (s)
Average	54	59
Median	53	54
Min	39	17
Max	76	119
Average deviation	9	29
Standard deviation	11	35
Variance	131	1199

small diameter act as a reserve, or emergency, routes for situations when large diameter tubes are damaged or the flow is blocked. We use this phenomenon of re-routing the flow to design logical gates. A detailed example of an XOR gate is shown in Fig. 2 and its scheme in Fig. 3a–d.

Flow is directed from '+' to '−' and then reversed from '−' to '+' (Figs. 2a and 3a). First order tubes *x* and *y* represent input Boolean variables. The second order tube *z* represents an output variable (Figs. 2a and 3a). If there is a flow of cytoplasm in a tube, the tube represent state *True*, if there is no flow state *False*. In an intact, or resting, state the gate's inputs are in state '1', tubes *x* and *y* exhibit flow of cytoplasm and tube *z* does not exhibit a flow: $x = 1$, $y = 1$, $z = 0$ (Figs. 2b and 3a). This is because tube *z*'s diameter, approx. 30 μm, is nearly three times smaller than the diameter of tubes *x* and *y*, approx. 100 μm.

When tube *x* is touched, as shown in Figs. 2c and 3b, tube *x* becomes 'non-conductive' and the flow through tube *x* stops. Subsequently, the pressure of cytoplasm increases and the cytoplasm

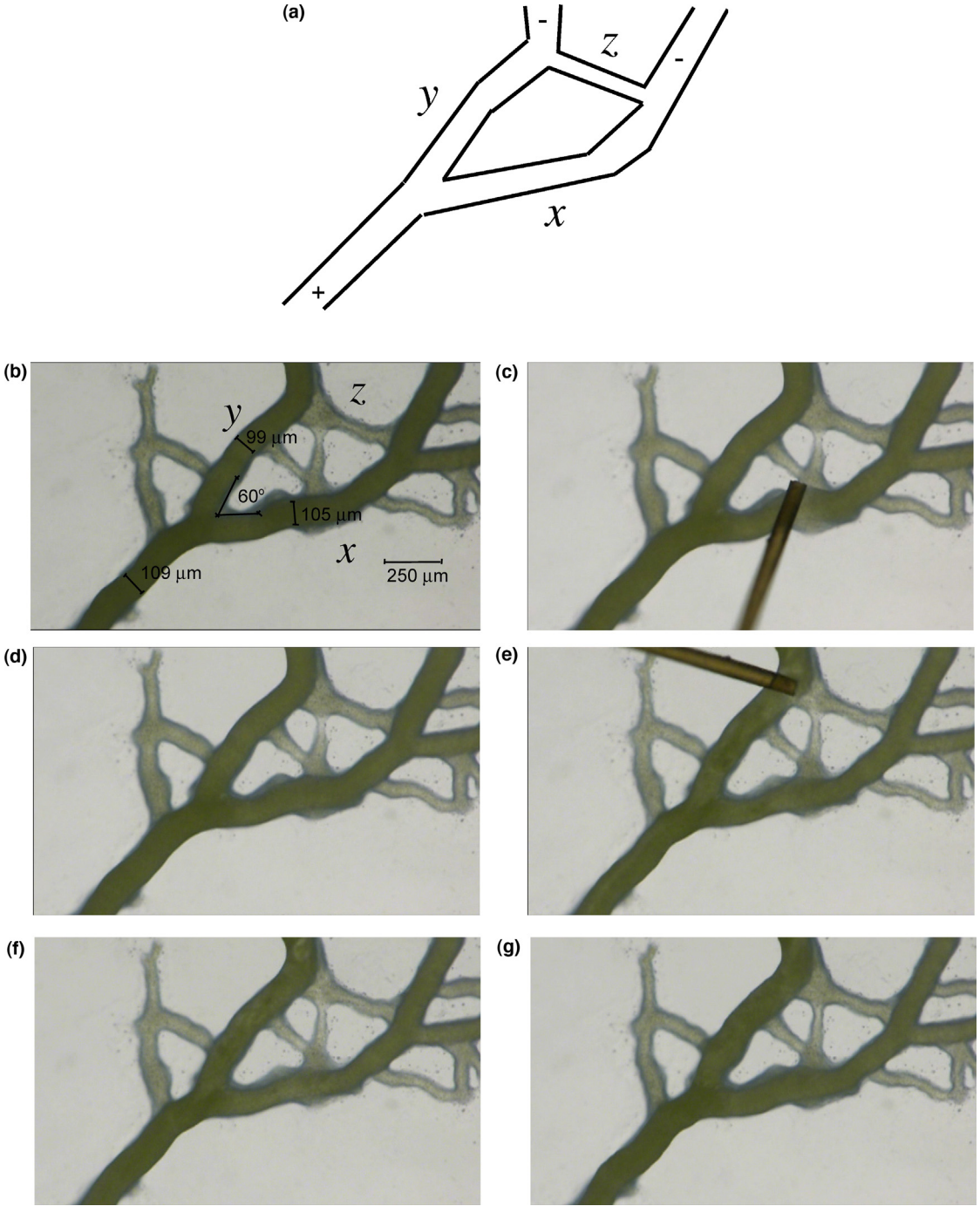

FIGURE 2

Implementation of an XOR gate in Physarum. (a) Scheme of the gate, input tubes *x* and *y* and output tube *z* are shown; '+' and '−' indicate polarity of cytoplasm flow, the polarity changes almost every minute, as per Table 1. (b) Snapshot of the living gate before stimulation: $x = 1$ and $y = 1$, $z = 0$; some parameters of the junction are indicated. (c) Mechanical stimulation of tube *x*, $x = 0$. (d) Gate after stimulation, $x = 0$, $y = 1$ and $z = 1$. (e) Mechanical stimulation of tube *y*, $y = 0$. (f) Gate after stimulation $x = 1$, $y = 0$, $z = 1$. (g) Gate restores itself to a 'resting' state $x = 1$, $y = 1$, $z = 0$.

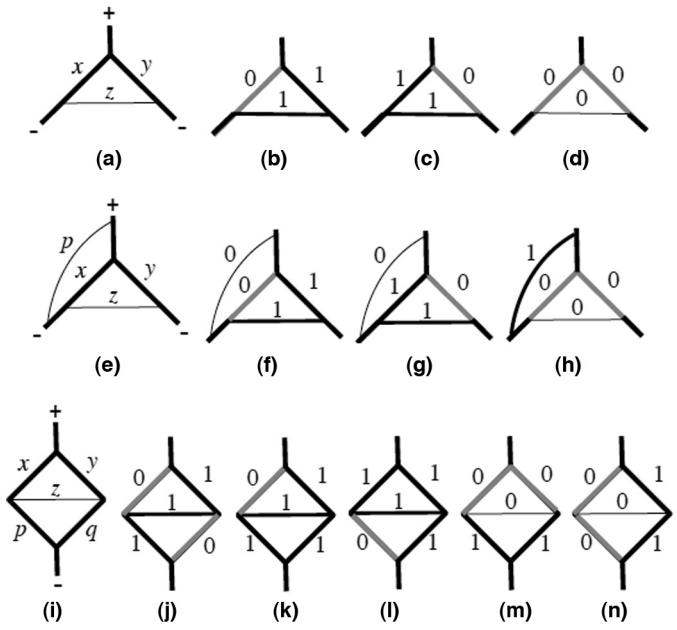

FIGURE 3

Schematics of gates implementable with Physarum tubes. Tubes x and y are solid black when representing logical *True*, $x = 1$, $y = 1$, and gray when representing logical *False*, $x = 0$, $y = 0$. Tubes z and p are thin when representing *False*, $z = 0$, $p = 0$ and are thick when representing *True*, $z = 1$, $p = 1$. Symbols '+' and '−' indicate polarity of the cytoplasm flow, the polarity changes almost every minute, as per Table 1. (a)–(d) XOR gate, discussed in Fig. 2, $z = x \oplus y$, where (a) $x = 1$, $y = 1$, (b) $x = 0$, $y = 1$, (c) $x = 1$, $y = 0$, (d) $x = 0$, $y = 0$. (e)–(h) XOR and NOR gates: $z = x \oplus y$ and $p = \overline{x + y}$, where (e) $x = 1$, $y = 1$, (f) $x = 0$, $y = 1$, (g) $x = 1$, $y = 0$, (f) $x = 0$, $y = 0$. (i)–(n) combined gate: $z = xy\,p + xyq + x\,pq + y\,pq$, where (i) $x = 1$, $y = 1$, $p = 1$, $q = 1$, (j) $x = 0$, $y = 1$, $p = 1$, $q = 0$, (k) $x = 0$, $y = 1$, $p = 1$, $q = 1$, (l) $x = 1$, $y = 1$, $p = 0$, $q = 1$. (m) $x = 0$, $y = 0$, $p = 1$, $q = 1$, (n) $x = 0$, $y = 1$, $p = 0$, $q = 1$.

is directed through tube z, the diameter of which increases to 70 υm due to pressure from the passing cytoplasm (Figs. 2d and 3b).

The gate remains in such a state for on average 54 s (Table 1) and then tube x restores its conductivity. The flow of cytoplasm is then directed through tubes x and y, and tube z becomes unused, shrinks due to elasticity and its diameter returns to a resting value 30 υm. This is somewhat analogous to an automated adjustment employed in a microfluidic implementation of a Wheatstone bridge [35]. The state of the gate after mechanical stimulation of tube y (Fig. 2e) is shown in Figs. 2f and 3c. The gate is restored to its original state in less than a minute after mechanical stimulation. When the flow stops in x and y at the same time the flow may not occur in tube z because the tube becomes isolated from the upper part of protoplasmic network. Therefore we assume that $z = 0$ if $x = 0$ and $y = 0$. Thus an XOR gate is implemented $z = x \oplus y$ (Fig. 3a–d).

By adding one more second order tubes to the XOR gate (Fig. 3a–d) we produce a gate with two inputs and two outputs (Fig. 3e–h). The gate is shown in (Fig. 3e–h). It computes exclusive disjunction and negated disjunction in parallel. The output tube $z = x \oplus y$ acts in a manner similar to an XOR gate (Fig. 3a–d). The output tube $p = \overline{x + y}$ connects the inlet to tube x, just before the junction of x and z, to the outlet of the junction of the tubes x and y. Cytoplasmic flow is directed via tube p, $p = 1$ only if tubes x and y are blocked, $x = 0$ and $y = 0$ (Fig. 3h).

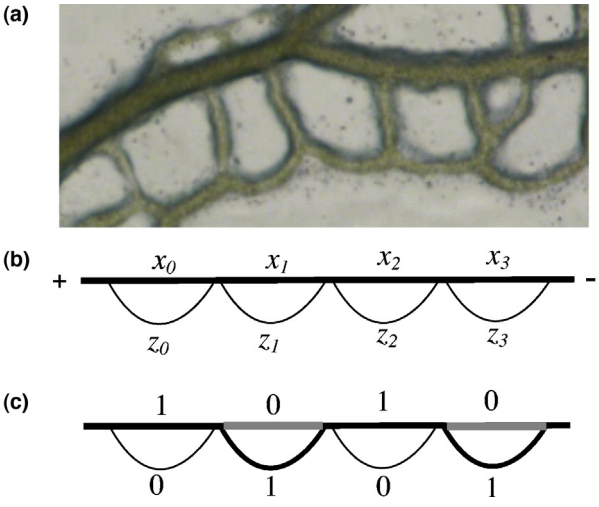

FIGURE 4

Rewritable memory. (a) Photo of living memory string. (b) and (c) Scheme of a memory string: $z_i = x_i$, $i = 0, \ldots, 3$, where (b) $x_i = 0$, $i = 0,\ldots,3$, (c) $x_0 = 1$, $x_1 = 0$, $x_2 = 1$, $x_3 = 0$. Signs '+' and '−' indicate polarity of cytoplasm flow, the polarity changes almost every minute, as per Table 1.

By adding two more first order tubs to the XOR gate (Fig. 3a–d) we produce a gate with four inputs and one output (Fig. 3i–n). The gate $z = \bar{x}y\,p + x\bar{y}q + x\,\bar{p}q + y\,p\bar{q}$ (Fig. 3i–n) responds with *True* only when one input tube is blocked and two of its neighboring input tubes are unblocked. Examples are as follows. Tubes x and q are blocked, $x = 0$ and $q = 0$, tubes y and p are unblocked, $y = 1$ and $p = 1$ (Fig. 3j), flow is directed via tube z. Tubes y, p, q are unblocked, $y = 1$, $p = 1$, $q = 1$, tube x is blocked, $x = 0$ (Fig. 3k), flow is directed via tube z. Tubes x, y and q are unblocked and tube p is blocked (Fig. 3l), flow is directed via tube z. For all other combination of input tuples, the output is *False*. Examples are as follows. Tubes x and y are blocked and tubes p and q are unblocked (Fig. 3m), there is no flow of cytoplasm through the gate and thus $z = 0$. Tubes x and p are blocked and tubes y and q are unblocked (Fig. 3n), cytoplasm flows through tubes y and q and thus $z = 0$.

A protoplasmic network of Physarum commonly exhibits the structures illustrated in Fig. 4a. A first order protoplasmic tube has a festoon of second order tubes. The second order tubes play the role of emergency bypasses and auxiliary pathways for distributed sensorial fusion, as well as the removal of metabolites. Using these structures we can implement binary memory arrays, see Fig. 4b,c. A memory string z is a bitwise inverse of an input string x. Thus to write an input string 0101 we mechanically stimulate fragments x_1 and x_3 (Fig. 4c). A cytoplasmic flow through x_1 and x_3 becomes blocked in a response to the stimulation. The cytoplasmic flow is then redirected via the route $x_0z_1x_2z_3$.

Discussion

We explored the topologies of Physarum protoplasmic networks and demonstrated that basic logical gates can be implemented in living slime *P. polycephalum*. The Physarum fluidic gates are synchronized by propagating calcium waves. Slime mold *P. polycephalum* is a living microfluidic device. Even the diameter of Physarum protoplasmic tubes, approx. 100 μm, matches the width of most common man-made microfluidic devices [12–14].

With Physarum we can implement growing microfluidic devices. Growing Physarum circuits can be controlled by light [36,37], spatial distribution of attractants and repellents and chemical gradients [38–41], temperature gradients [42] and electrical fields [43]. Embedded logical gates constructed with living slime mold make a substantial contribution to the development of Physarum-based computing devices. In 2001 Nakagaki et al. [44] showed that the topology of the plasmodium's protoplasmic network optimizes the plasmodium's harvesting of nutrient resources from the scattered sources of nutrients and makes the transport of intra-cellular components more efficient. In [25] we showed how to construct specialized and general purpose massively parallel amorphous computers from *P. polycephalum* that are capable of solving problems of computational geometry, graph-theory and logic. Microfluidic logic gates that have been developed complement, but do not yet substitute previously designed prototypes of Physarum logical gates based on chemo-attraction [45] and collision-based (or ballistic) computing [25,46].

A need for mechanical control is hereditary to many microfluidic circuits, and slime mold circuits are not an exception. In principle, Physarum fluidic gates can be cascaded using opto-mechanical coupling, e.g. the width of an output tube or the speed of flow in the output tube could be detected by optical means and the input tubes of subsequent gates could be stimulated mechanically, though this is not an optimal solution.

Another implementation, as suggested by the referees, would be to add a thin tube to an output so that cytoplasm flow in gate-tubes can be controlled by the added tube. There is a problem though: Physarum tubes usually merge when they touch each other. Thus tubes touching each other should be insulated. Any insulation will restrict peristaltic activity of the tubes and thus might impair functioning of the gates.

Further thought is required on how to exploit the mechanical properties of slime mold tubes to make device-embedded flow switching functions. There are some published results showing that embedded check valves and switch valves (with pressure-dependent states), analogous to diode and p-channel JFET transistor, can be implemented in layered elastomeric materials [18]. Another route to explore could be to map designs of hybrid fluidic–electronic–mechanical universal logical gates [19,20] onto patterns of living slime mold devices. With respect to the delivery of (e.g.) encapsulated substances by plasmodial tubes, changes in the cytoplasmic resistance in tubes containing capsules can be exploited to construct logical gates similar to droplet based gates [16] and bubble logic systems [17].

Physarum microfluidic gates are slow: their speed is on the order of seconds, much slower than silicon gates. However, slime mold microfluidic gates are self-growing and self-repairing and can be incorporated into hybrid wetware: hardware devices for sensing and analyzing non-lethal substances, and the detection of molecules or certain types of living cell [47]. The Physarum microfluidic gates could form the basis for disposable biocompatible mechanically controlled devices [48], as embedded fluidic controllers and circuits in bio-inspired robots [49] or memory arrays [22,23] embedded into soft-bodied robots.

In terms of real life speed, Physarum fluidic gates cannot compete with silicon-based circuits, yet they are compatible with other unconventional implementations of logical circuits: adders based on fingers growing in liquid crystals, logical gates in excitable chemical medium, crystallization based gates and crab based gates. Also, the Physarum gates offer a high-density of basic logical elements to be implemented on a planar substrate. Assuming that every junction of protoplasmic tubes can be utilized as a logical element we can estimate that there will be approx. 10–20 elementary computing units on 1 mm by 1 mm of planar substrate (Fig. 5).

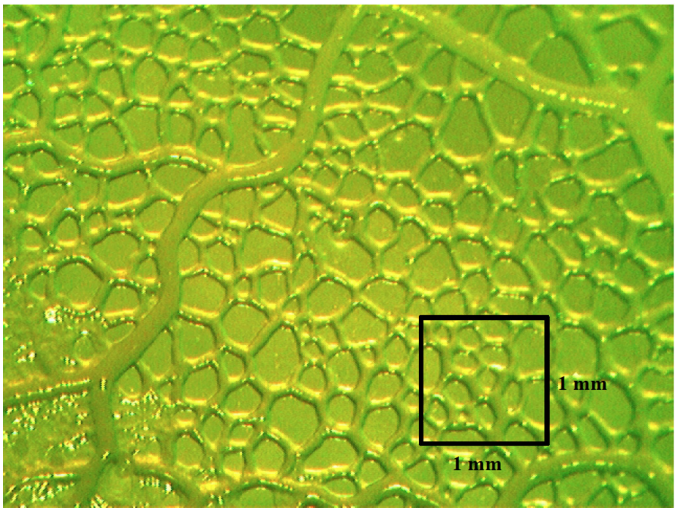

FIGURE 5

Photograph of dense protoplasmic network with 1 mm by 1 mm. The network is grown on a nutrient agar gel.

Acknowledgement

We thank Dr. Holger Kletti (Faculty of Engineering, Bauhaus-University Weimar) for his help with microscopic techniques.

Appendix A. Supplementary data

Supplementary material related to this article can be found, in the online version, at doi:10.1016/j.mattod.2014.01.018.

References

[1] R.D. Allen, et al. Science (142) (1963) 1485–1487.
[2] A.V. Bykov, et al. J. Biophotonics 2 (2009) 540–547.
[3] W. Gawlitta, et al. Cell Tissue Res. 209 (1980) 71–86.
[4] N. Hulsmann, K.E. Wohlfarth-Bottermann, Cytobiologie 17 (1978) 317–334.
[5] S.A. Newton, et al. Biochem. Biophys. Acta 496 (1977) 212–224.
[6] P.A. Stewart, B.T. Stewart, Exp. Cell Res. 18 (1959) 374–377.
[7] A. Adamatzky, Mater. Sci. Eng. C 30 (2010) 1211–1220.
[8] H.S. Li, D.B. Stolz, G. Romero, Traffic 6 (2005) 324–334.
[9] V. Müller, J.D. Köhler, T.U. Homann, FEBS Lett. 586 (2012) 3626–3632.
[10] R.J. Goodall, J.E. Thompson, Exp. Cell Res. 64 (1971) 1–8.
[11] R. Mayne, et al. Int. J. Nanotechnol. Mol. Comput. 3 (3) (2013) 1–14.
[12] B. Kirby, Micro- and Nanoscale Fluid Mechanics: Transport in Microfluidic Devices, Cambridge University Press, 2010.
[13] D.W.M. Marr, T. Munakata, Commun. ACM 50 (2007) 64–68.
[14] P. Tabeling, Introduction to Microfluidics, University Press, 2010.
[15] D. van Noort, Y. Yang, 15th International Conference on Miniaturized Systems for Chemistry and Life Sciences, October 2–6, Seattle, WA, USA, 2011.
[16] L.F. Cheow, L. Yobas, D.L. Kwong, Appl. Phys. Lett. 90 (2007) 054107.
[17] M. Prakash, N. Gershenfeld, Science 315 (2007) 832–835.
[18] B. Mosadegh, et al. Nat. Phys. 6 (2010) 433–437.
[19] M. Zhang, et al. Soft Matter 7 (2011) 7493–7497.
[20] B. Zhou, et al. Lab Chip 7 (2011) 7493–7497.
[21] M.W. Toepke, V.V. Abhyankar, D.J. Beebe, Lab Chip 7 (2007) 1449–1453.
[22] A. Groisman, M. Enzelberger, S.R. Quake, Science 300 (2003) 955–958.

[23] A. Groisman, S.R. Quake, Phys. Rev. Lett. 92 (2004) 094501.
[24] T. Vestad, D.W.M. Marr, T. Munakata, Appl. Phys. Lett. 84 (2004) 5074–5075.
[25] A. Adamatzky, Physarum Machines, World Scientific, 2010.
[26] L.V. Heilbrunn, K. Daugherty, Physiol. Zool. 12 (1939) 1–12.
[27] W. Seifriz, Science 86 (1937) 397–402.
[28] J. Fingerle, D. Gradmann, J. Membr. Biol. 68 (1982) 67–77.
[29] R. Meyer, W. Stockem, Cell Biol. Int. Rep. 3 (1979) 321–330.
[30] T. Iwamura, Bot. Mag. 62 (1949) 126–131.
[31] N. Kamiya, S. Abe, J. Colloid Sci. 5 (1950) 149–163.
[32] U. Kashimoto, J. Gen. Physiol. 41 (1958) 1205–1222.
[33] O.P. Hamil, B. Martinac, Physiol. Rev. 81 (2001) 685–740.
[34] R.D. Kamm, M.R. Kaazempur-Mofrad, Mech. Chem. Biosyst. 1 (2004) 201–209.
[35] M. Tanyeri, et al. Lab Chip 11 (2011) 4181–4186.
[36] A. Adamatzky, Steering plasmodium with light: dynamical programming of Physarum machine, 2009 arxiv:0908.0850.
[37] D.P. Hader, T. Schreckenbach, Plant Cell Physiol. 25 (1) (1984) 55.
[38] A. Adamatzky, IEEE Trans. NanoBiosci. 11 (2012) 131–134.
[39] A. Adamatzky, P.P.B. de Oliveira, Kybernetes 40 (2011) 1373–1394.
[40] A. Adamatzky, M. Prokopenko, Int. J. Parallel Emerg. Distribut. Syst. 27 (2012) 275–295.
[41] D.J.C. Knowles, M.J. Carlile, J. Gen. Microbiol. 108 (1) (1978) 17.
[42] R. Wolf, J. Niemuth, H. Sauer, Protoplasma 197 (1) (1997) 121–131.
[43] S. Tsuda, et al. Int. J. Nanotechnol. Mol. Comput. 3 (2011) 2.
[44] T. Nakagaki, H. Yamada, A. Toth, Biophys. Chem. 92 (2001) 47–52.
[45] S. Tsuda, M. Aono, Y.P. Gunji, BioSystems 73 (2004) 45–55.
[46] J. Jones, A. Adamatzky, BioSystems 101 (2010) 51–58.
[47] B. De Lacy Costello, A. Adamatzky, Commun. Integr. Biol. 6 (2013) e25030.
[48] W. Li, et al. Lab Chip 12 (2012) 1587.
[49] C. Melhuish, A. Adamatzky, B.A. Kennedy, SPIE Proceedings, Smart Structures and Materials. Electroactive Polymer Actuators and Devices, vol. 4329, Yoseph Bar-Cohen, 2001, pp. 16–27.